Int. J. Solids Structures Vol. 15, pp. 379–393

0020-7683/79/0501-0379/$02.00/0

A NUMERICAL STUDY OF NECKING IN THE PLANE TENSION TEST

M. A. BURKE† and W. D. NIX‡

Department of Materials Science and Engineering, Stanford University, Stanford, CA 94305, U.S.A.

(*Received* 28 *June* 1978; *in revised form* 15 *August* 1978; *received for publication* 31 *October* 1978)

Abstract—The boundary value problem for the plane-strain uniaxial tension of a rectangular bar is posed in two ways. In one case the ends of a specimen of compressible elastic–plastic material are assumed to remain shear free. Uniform deformation is terminated by an abrupt bifurcation. The eigenvalue problem governing bifurcation which is based on Hill's variational statement of uniqueness is solved by means of the finite element method. An updating Lagrangian formulation for large elastic–plastic strain is employed. The influence of the rate of work hardening and the specimen slenderness ratio on the bifurcation point is studied and a comparison is made with the conventional engineering criterion for stability. The post bifurcation behavior is then determined. Here the computations along with those for the second case, which considers the entire deformation history of a bar cemented to rigid grips, are based on a variational form of the rate equilibrium equations. The effect of end conditions on the deformations in the necked down bar is assessed.

1. INTRODUCTION

The conventional criterion for stability in a tension test[1] suggests that necking will be initiated at the point where a maximum is reached in the load supported by the specimen. This result pertains to time independent elastic–plastic material behavior. Recently, Burke and Nix[2] reviewed an extension of this criterion to the case of rate sensitive materials in tension creep tests. Stability, in these instances, was associated with the nature of the relative rate of area reduction between an already perturbed or necked region and the unaffected geometrically uniform part.

A more complete criterion should examine the mode of the perturbation itself and be based on energy considerations. A criterion for stability in a dynamical sense which pertains to finite time independent deformation has been established by Hill[3]. In addition, Hill has shown that the condition of stability is closely related to that of uniqueness of the deformation field for a particular boundary value problem.

Isothermal deformation of a solid body is normally accompanied by some change in loading when the material law is time independent. Specifically, for finite deformation, the loads on certain surface elements generally vary in magnitude or direction during additional straining. As has been made evident in analyses which employ Hill's variational principle for uniqueness, there are exceptional configurations where the nominal traction vectors are momentarily constant as the body is incrementally deformed in particular ways. The instantaneous velocity fields are then nontrivial solutions of a homogeneous boundary value problem, and may be termed eigenmodes and the corresponding structural–material state, the eigenstate[4–7]. It has recently been demonstrated that eigenstates exist for certain tension tests with particular boundary conditions and that a necking mode is one form of incremental deformation which can occur[8–12]. It has been further demonstrated in these cases that necking is postponed and uniform deformation persists often times well beyond the point at which the maximum load was attained.

The purpose of this paper is to present results of a numerical study of the bifurcation phenomenon in a plane-strain tension test. The deformation is finite, compressible and elastic–plastic in nature. The influence of the specimen slenderness ratio and the rate of strain hardening on the point of instability is examined. A post bifurcation analysis is also performed which describes the initiation and growth of a neck. A study is also made of the behavior of a tension specimen which necks, not as the result of a sudden bifurcation, but in a continuous manner, due to the non-uniform deformation that results when rigid grips are used. The rate of

†M. A. Burke, formerly Graduate Research Assistant at Stanford is now Senior Engineer at Marc Analysis Research Corporation, Palo Alto, CA 94306, U.S.A.

‡W. D. Nix is Professor of Materials Science and Engineering at Stanford University.

growth of the neck and the elastic–plastic regions are compared with the results for the deformation of a specimen with shear-free end conditions. The bifurcation point which will be determined corresponds to the primary eigenstate or first possible instability which can occur along a given strain path that passes through a sequence of equilibrium states starting from the initial unloaded state.

2. A REVIEW OF THE VARIATIONAL PRINCIPLE

In his development of the variational formulations, Hill[4] considers a class of time independent material behavior in which the stress rates are derivable from a homogeneous potential function of degree two in the velocity gradients according to the relationship

$$\dot{S}_{ij} = \frac{\partial E}{\partial(\partial v_j/\partial X_i)} \tag{1}$$

where S_{ij} is a component of the unsymmetric nominal stress tensor. Any solution of a boundary value problem, unique or not, can be characterized by a variational principle, namely that

$$I = \int_{V^0} E\left(\frac{\partial v_j}{\partial X_j}\right) \mathrm{d}V^0 - \int_{S_F^0} \dot{F}_j v_j \,\mathrm{d}S^0 - \int_{V^0} \dot{g}_j v_j \,\mathrm{d}V^0 \tag{2}$$

is stationary in the class of continuous differentiable velocity fields which assume the values that are prescribed over S_V^0; the complete surface, S^0, is comprised of a segment S_F^0 over which traction rates are prescribed and the complementary portion, S_V^0. The typical traction boundary condition considered here is that the change in the "load" vector on an infinitesimal surface element is assigned, irrespective of changes in its area and orientation. Then at any stage t there is given, not the rate of change of the "true" traction, but the rate of change of the "nominal" traction, $\dot{F}_j$, based on the configuration at that instant. Also, $\dot{g}_j$ is the body force rate per unit initial volume and V^0 is the reference volume of the body. The first variation of eqn (2) with respect to kinematically admissible velocity fields, δv_j, will vanish, when $\delta v_j = 0$ on S_V^0.

Plastic flow is essentially a fluid type phenomenon which can be expressed most conveniently in terms of the current configuration of the material. The finite strain formulation which will be employed treats the reference or initial configuration as coincident with the current configuration at time t. The initial invariant reference is rectangular Cartesian, X_i. If the position of particles in the deformed body are also expressed in Cartesian coordinates, x_i, then

$$x_i = x_i(\mathbf{X}, T) \tag{3}$$

and by the device of treating both configurations as instantaneously coincident

$$X_i = x_i(\mathbf{X}, t). \tag{4}$$

The governing variational principle can then be expressed as

$$\int_V \dot{S}_{ij}\delta\frac{\partial v_j}{\partial x_i}\,\mathrm{d}V - \int_{S_F} \dot{F}_i \delta v_i \,\mathrm{d}S - \int_V \dot{g}_i \delta v_i \,\mathrm{d}V = 0 \tag{5}$$

where S, V are the current surface and volume respectively. The velocity and stress rate distributions at time t are found by solution of the above variational equality and are used to determine the increments of stress and displacement that occur over the interval Δt. The time increment or corresponding applied displacement increment is sufficiently small that piecewise linear relations hold between field variables.

3. CONSTITUTIVE RELATIONS

The use of the stress rate tensor $\dot{S}_{ij}$ in eqn (5) is convenient when rotations are substantial during finite deformation; also, as will be shown subsequently, it is convenient when the stress

magnitudes are of the same order as the rate of work hardening. It is not the stress rate tensor which is found in any constitutive relation as it contains the effect of a stress change due to rigid body rotations. What is usually measured or derived from measurements in a typical tension test, is the material rate of change of the Cauchy stress. The stress tensor σ_{ij} is expressed in terms of rectangular coordinates in the current configuration. There is no rotation of material elements in such a test. When rotations occur an objective or spin invariant rate for the Cauchy stress tensor, σ_{ij}, is the Jaumann derivative $\mathcal{D}/\mathcal{D}t$. It is the rate of change associated with a set of coordinates that translates and rotates with the material[13, 14]. The relation between the material derivative and the Jaumann derivative of the Cauchy stress in terms of the current rectangular coordinates is given by the following

$$\frac{\mathcal{D}\sigma_{ij}}{\mathcal{D}t} = \dot{\sigma}_{ij} - W_{ik}\sigma_{kj} - W_{jk}\sigma_{ki} \tag{6}$$

where W_{ij} are the components of the spin tensor or antisymmetric part of the velocity gradient,

$$W_{ij} = \frac{1}{2}\left(\frac{\partial v_i}{\partial x_j} - \frac{\partial v_j}{\partial x_i}\right). \tag{7}$$

The components of the symmetric part of the velocity gradient, or rate of deformation tensor are

$$D_{ij} = \frac{1}{2}\left(\frac{\partial v_i}{\partial x_j} + \frac{\partial v_j}{\partial x_i}\right). \tag{8}$$

The relation between the nominal stress tensor and the Cauchy stress tensor in terms of the current rectangular Cartesian coordinates, x_i, is given by

$$\mathbf{FS} = J\boldsymbol{\sigma}. \tag{9}$$

Here, $J = \rho^0/\rho$ is the Jacobian of the transformation from the initial state to the deformed state, and ρ^0, ρ are the initial and final densities of a material element. The deformation gradient is denoted by **F**.

If the material derivative of eqn (9) is taken and the result is particularized to the case of coincident reference and current configurations where F and J are unity, then

$$\dot{S}_{ij} + S_{kj}\frac{\partial v_i}{\partial x_k} = \sigma_{ij}\frac{\partial v_k}{\partial x_k} + \dot{\sigma}_{ij}. \tag{10}$$

In this case, the nominal stress components, S_{ij}, are equal to the Cauchy or true stress components, σ_{ij}. This leads to the expression

$$\dot{S}_{ij} = \left(\frac{\mathcal{D}\sigma_{ij}}{\mathcal{D}t} + \sigma_{ij}\frac{\partial v_k}{\partial x_k}\right) - (\sigma_{ij}D_{jk} + \sigma_{ij}D_{ik}) + \sigma_{ij}\frac{\partial v_j}{\partial x_k}. \tag{11}$$

It follows from eqn (1) that the r.h.s. of the above equality is derivable from the homogeneous potential function E. Now experimental results can describe a constitutive behavior in the form[15]

$$\frac{\mathcal{D}\sigma_{ij}}{\mathcal{D}t} = L_{ijkl}D_{kl}. \tag{12}$$

When the deformation is strictly elastic and infinitesimal, the coefficients L_{ijkl} are based on generalizations from Hooke's Law. When deformation is elastic–plastic, the slope of the stress-plastic strain curve is also required and the tensor of moduli are derivable from the inverted Prandtl–Reuss flow equations for isotropically work hardening material and, for

example, the Von Mises yield criterion. Unfortunately these coefficients are not derivable from a potential function in the large strain regime. The reasons for requiring the existence of E or the desired related function for $\mathscr{D}\sigma_{ij}/\mathscr{D}t$, in Hill's terminology[5] were to make the field equations self-adjoint, so that all solutions to inhomogeneous self-adjoint boundary-value problems are characterized by a variational principle. The use of the constitutive relation (12) in the development of a finite element formulation will result in an unsymmetric stiffness matrix.

If the potential function, E, exists, it can be shown that a related homogeneous function of degree two exists for the Kirchhoff stress rates $\mathscr{D}\tau_{ij}$ in terms of the rate of deformation. The relation between the stress rates is given by

$$\frac{\mathscr{D}\tau_{ij}}{\mathscr{D}t} = \frac{\mathscr{D}\sigma_{ij}}{\mathscr{D}t} - \sigma_{ij}\frac{\partial v_k}{\partial x_k} \tag{13}$$

when the reference and current configurations are coincident. A logical extension which uses the Prandt–Reuss equations and which can be incorporated into the variational formulation is obtained[16] by replacing $\mathscr{D}\sigma_{ij}/\mathscr{D}t$ with $\mathscr{D}\tau_{ij}/\mathscr{D}t$. Following the work of Hutchinson[17], it is assumed that eqn (12) now is taken to be

$$\frac{\mathscr{D}\tau_{ij}}{\mathscr{D}t} = L_{ijkl}D_{kl}, \tag{14}$$

where

$$L_{ijkl} = 2G\left[\delta_{ik}\delta_{jl} + \frac{\nu}{1-2\nu}\delta_{ij}\delta_{kl} - \frac{\sigma'_{ij}\sigma'_{kl}}{\Phi}\right]. \tag{15}$$

Here, G is the shear modulus, γ is Poisson's ratio, δ_{ij} is the Kronecker delta, and σ'_{ij} are the deviatoric components of stress. The function Φ is given by

$$\Phi = \frac{2}{3}\bar{\sigma}^2\left(1+\frac{h}{3G}\right) \tag{16}$$

where $\bar{\sigma}$ is the Von Mises effective Cauchy stress and h is the current slope of the true stress-natural plastic strain curve.

The moduli have two branches. The above set applies when elastic-plastic loading occurs (i.e. $\bar{\sigma} = \bar{\sigma}_F$ and $\dot{\bar{\sigma}} \geqslant 0$, where $\bar{\sigma}_F$ is the current yield or flow stress). When elastic loading or unloading occurs (i.e. $\bar{\sigma} < \bar{\sigma}_F$ or $\bar{\sigma} = \bar{\sigma}_F$ but $\dot{\bar{\sigma}} < 0$) the last term in the above brackets is dropped. This constitutive law is equivalent to the commonly used elastic–plastic constitutive description (12) to within terms of stress divided by elastic modulus since the volume change is taken to be purely elastic. Lee[18] has observed that eqn (14) provides a better approximation to the nonlinear elastic behavior of metals even when the moduli are still formed from the two classical elastic constants according to Hooke's Law.

4. THE FINITE ELEMENT FORMULATION

An expression for the nominal stress rate in terms of the Jaumann rate of Kirchhoff stress can be obtained by substituting eqn (13) into (11); hence

$$\dot{S}_{ij} = \frac{\mathscr{D}\tau_{ij}}{\mathscr{D}t} - (\sigma_{jk}D_{ik} + \sigma_{ki}D_{ik}) + \sigma_{ij}\frac{\partial v_j}{\partial x_k}. \tag{17}$$

Thus, the potential function E can now be written as

$$E\left(\frac{\partial v_i}{\partial x_i}\right) = \frac{1}{2}\frac{\mathscr{D}\tau_{ij}}{\mathscr{D}t}D_{ij} - \frac{1}{2}\sigma_{ij}\left(2D_{ik}D_{jk} - \frac{\partial v_k}{\partial x_i}\;\frac{\partial v_k}{\partial x_j}\right) \tag{18}$$

and the variational principle as

$$\int_V\left[\frac{\mathscr{D}\tau_{ij}}{\mathscr{D}t}\delta(D_{ij}) - \frac{1}{2}\sigma_{ij}\delta(2D_{ik}D_{kj} - v_{k,i}v_{k,j})\right]\mathrm{d}V - \delta\left(\int_{S_F}\dot{F}_i v_i\,\mathrm{d}S + \int_V \dot{g}_i v_i\,\mathrm{d}V\right) = 0 \tag{19}$$

The stress tensor of interest is the Cauchy or true stress at a material point and this is computed for the updated current coordinates by

$$\sigma(t+\Delta t) = \sigma(t) + \dot{\sigma}\Delta t \tag{20}$$

where $\dot{\sigma}$ is the material derivative for a particle. The relation between this stress rate and the rate $\mathcal{D}\tau/\mathcal{D}t$ given above is found by combining eqns (6) and (13). Hence,

$$\dot{\sigma}_{ij} = \tau^{*}_{ij} - \sigma_{ij}\frac{\partial v_k}{\partial x_k} + W_{ik}\sigma_{kj} - \sigma_{ik}W_{kj}. \tag{21}$$

The potential E differs from the small strain potential $W(\dot{\epsilon}_{ij})$ essentially by the inclusion of the second term in eqn (18). This latter term accounts for rotational effects in finite deformation. However, McMeeking and Rice [19] have pointed out the importance of this term even in the absence of rotations. Denoting strain rate as $\dot{\epsilon}$, then the first term in eqn (19) is proportional to $h\dot{\epsilon}_2^2$. The second term, proportional to $\sigma\dot{\epsilon}^2$, can be significant particularly in materials which exhibit low strain hardening rates.

The variational equality (19) is discretized by means of the finite element method. This yields the following matrix formulation

$$\{\delta v\}^T\left\{\int_V [B]^T[L][B]\,dV + \int_V ([N_k],_i^T\sigma_{ij}[N_k],_i - 2[B_{ki}]^T\sigma_{ij}[B_{jk}])\,dV - \int_{S_F}[N]^T\{\dot{F}\}\,dS + \int_V [N]^T\{\dot{g}\}\,dV\right\} = 0 \tag{22}$$

where $i, j, k = 1, 2$. Here, $\{v\}$ are the nodal displacement rates, $[L]$ is the matrix form of eqn (15), and $[N]$ is the matrix of interpolating functions. The 8-node planar isoparametric element [20] will be used. $[B_{ij}]$ is a row of the conventional (infinitesimal strain) strain rate-nodal velocity matrix which produces D_{ij} (8). The first integral in the above expression is the conventional stiffness matrix for small strain elastic–plastic formulations [21]. The second integral is referred to as the initial stress matrix [19].

5. BIFURCATION ANALYSIS

A sufficient condition for uniqueness exists when

$$\int_V \dot{\tilde{S}}_{ij}\frac{\partial \tilde{v}_i}{\partial x_j}\,dV > 0 \tag{23}$$

where the tilde denotes the difference between corresponding quantities. However, a problem arises in applying the uniqueness criterion when the material deforms plastically [22]. Due to the nonlinearity inherent in the different behavior in loading and unloading, the differences in the stress rates, $\dot{\tilde{S}}_{ij}$ cannot be related to the differences in the velocity gradients, $\partial\tilde{v}_i/\partial x_j$, by the linear relation (1). Nevertheless, by choosing what is termed a linear comparison solid that displays identical behavior to the actual elastic–plastic material in certain regions of strain rate space, a lower bound can be determined for the point of non-uniqueness and instability.

It can be shown [23] that the function E (18) can be decomposed as $Q + R$. The potential, Q, for the comparison solid is given by

$$Q = D_{ij}\xi_{ijkl}D_{kl} - \frac{1}{g}(\lambda_{kl}D_{kl})^2 + \sigma_{ij}\left(\frac{\partial v_k}{\partial x_i}\frac{\partial v_k}{\partial x_j} - 2D_{ij}D_{jk}\right) \tag{24}$$

where ξ_{ijkl} is the tensor of elastic moduli and, λ_{kl} is the normal to the hyperplane interface between elastic and plastic domains in strain rate space. The function g depends on the current plastic flow properties and is given by

$$g = h + \lambda_{ij}\mu_{ij} \tag{25}$$

where μ_{ij} is the normal to the interface in stress rate space. To complete the decomposition of E, the function R must then have the convex form

$$R = \frac{1-\alpha}{2g}(\lambda_{kl}D_{kl})^2 \tag{26}$$

where $\alpha = 1$ or 0 depending on whether $\lambda_{kl}\, D_{kl}$ is positive or negative.

The eigenmode for the comparison solid can then be directed arbitrarily into the half space $\lambda_{kl}D_{kl} \geq 0$ by choosing its amplitude to be of the proper sign. In which case $\alpha = 1$, $R = 0$, and the behavior of the actual solid and the comparison solid is identical. Since

$$\int_V Q\left(\frac{\partial \tilde{v}_i}{\partial x_i}\right) \mathrm{d}V \geq 0 \tag{27}$$

the first variation vanishes with respect to any field that makes this functional zero. Hence the bifurcation eigenvalue problem can be expressed by the variational equality

$$\delta \int_V Q\left(\frac{\partial \tilde{v}_i}{\partial x_i}\right) \mathrm{d}V = 0 \tag{28}$$

or

$$\int_V \left[\frac{\mathscr{D}\tilde{\tau}_{ij}}{\mathscr{D}t}\,\delta(\tilde{D}_{ij}) - \frac{1}{2}\sigma_{ij}\delta(2\tilde{D}_{ik}\tilde{D}_{kj} - \tilde{v}_{k,i}\tilde{v}_{k,j})\right] \mathrm{d}V = 0 \tag{29}$$

where $\tilde{D}_{ij}$ is related to $\tilde{v}$ through eqn (8) and $\mathscr{D}\tau_{ij}/\mathscr{D}t$ is related to $\tilde{D}_{ij}$ through eqn (14). Furthermore, by considering continued loading at the bifurcation point[13–24], the integrand of (29) is a lower bound to (23) and the primary eigenstate will be determined.

Since the fundamental solution and the bifurcation solution must both satisfy the displacement rate boundary conditions on S_v, the eigenmode which is the normalized difference between these solutions must satisfy the homogeneous boundary condition.

$$\tilde{v} = 0 \quad \text{on} \quad S_v. \tag{30}$$

The question then arises as to whether the bifurcation point is a stable equilibrium state. At this point assume that the body is set in motion by a transitory dynamic disturbance with kinetic energy ΔK^0. Then, at any instant following the disturbance

$$\Delta K = \Delta K^0 - \Delta U \tag{31}$$

where ΔU is the net energy representing the difference between the total internal work of distortion and the work done on the body by the external loads which are held constant during this free motion. This quantity which is expressed by the relation

$$\Delta U = \int_V \left\{\int \delta S_{ij}\, \mathrm{d}\left(\frac{\partial u_i}{\partial x_i}\right)\right\} \mathrm{d}V \tag{32}$$

must be positive, i.e. a body can depart from a stable equilibrium state only at the expense of the kinetic energy obtained from the disturbance. The inner integral of (32) is over any kinematically admissible path, **u**, which satisfies the homogeneous boundary conditions (30). The term δS_{ij} is the amount by which nominal stress differs from the equilibrium value at the end of a time interval δt.

Hill[3] has shown that over the path which is optimum, in the sense of not underestimating the least energy absorbed,

$$\Delta U = \frac{1}{2}(\delta t)^2 \int_V \dot{S}_{ij}\frac{\partial v_i}{\partial x_i}\,\mathrm{d}V. \tag{33}$$

The criterion for stability can then be expressed as

$$\int_V E\left(\frac{\partial v_i}{\partial x_j}\right) \mathrm{d}V > 0 \tag{34}$$

for the class of elastic–plastic solids under consideration. Recall that the integrand of (29) was made single-valued by considering only continued plastic loading at the bifurcation point. Hence, the criterion for uniqueness and stability of the linear comparison solid are synonymous in this case.

6. THE NUMERICAL PROCEDURE

Several possibilities exist to describe the boundary conditions for a tension test. One possibility is that a uniform axial displacement rate is prescribed at the ends of a specimen and these ends are cemented to rigid grips. This case is treated in the present study. Here, deformation is nonuniform and necking initiates immediately with loading.

Another possibility is that the boundary conditions consist of a prescribed nominal traction rate normal to the ends of the specimen. Then, immediately after the maximum load point, provided the prescribed value of traction rate is negative, there exist two solutions, one corresponding to continued uniform plastic loading, and the other to uniform elastic unloading. Thus, there is a rather trivial breakdown of uniqueness in this case. Finally, there is the situation where uniform axial displacement rates are prescribed along the ends of the specimen and these ends remain shear-free. In this case, one solution, corresponding to a state of uniform uniaxial stress, is available for all values of extension. This fundamental solution is unique for sufficiently small values of displacement. At some critical extension, a bifurcation from the fundamental solution first becomes possible.

At the bifurcation point, the complete (initial post-bifurcation) solution to the incremental boundary value problem is a linear combination

$$\Delta u_i = \Delta u_i^F + \xi \Delta u_i^E. \tag{35}$$

Here, Δu_i^F is the increment in the fundamental solution and Δu_i^E is the necking eigenmode from (29) and (30), regarded as normalized in some suitable fashion. The amplitude ξ must be chosen so that loading occurs everywhere in the current plastic zone for Δu_i. The nature of the initial necking mode was such that plastic flow is localized in a central region of the specimen while the remainder has a tendency to unload starting from a point on the axis of the specimen at the end of the bar. This was determined by assigning an arbitrarily small increment of uniform displacement following bifurcation and trying several values for the constant amplitude. The values of $\Delta\sigma_e$, the increment in effective stress, were then determined in each case and for all points in the body. The value of ξ which was chosen to initiate the post-bifurcation analysis was such that the minimum value of $\Delta\sigma_e$ at the point of intersection of the axis and the end of the bar was zero. This point then underwent neutral loading in the initial increment. Following the bifurcation point, the incremental solutions for the specimen with shear-free ends and the entire calculation of the deformation history of the specimen cemented to rigid grips are based on the variational equation of equilibrium given by (19).

The eigenvalue problem was solved numerically by the finite element method. The variational equation (29) is merely a special form of (19) without traction and body force terms. The discretized formulation given by (22) can therefore be used here. When the homogeneous boundary conditions are imposed, the variational equation becomes

$$[A(U_c)]\{\Delta U^E\} = 0 \tag{36}$$

where the symmetric matrix $[A]$ is the assembled stiffness matrix. Due to the symmetry of the deformation of a rectangular bar only one quadrant need be examined. The quadrant was discretized using the 5×15 mesh illustrated in Fig. 1.

To begin the bifurcation calculation, an initial guess is made for the critical extension, U_c. The material is assumed to deform uniformly in the x_3 plane under a small applied displacement

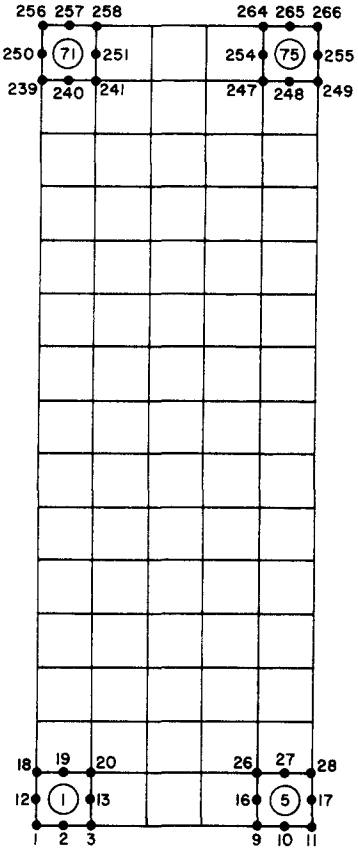

Fig. 1. Discretized quadrant of a rectangular tension specimen.

increment, ΔU_2, in the x_2 direction. Then for plane strain behavior, the nonzero stresses are σ_{22}, σ_{33} and the nonzero strain increments are ΔD_{11}, ΔD_{22}. Quantities prefaced with a Δ are rates multiplied by Δt. If the current configuration (L_1, L_2) and stress state $(\sigma_{22}, \sigma_{33})$ are known, then the updated values of these variables, are found as follows:

$$\Delta D_{22} = \frac{\Delta U_2}{L_2}. \tag{37a}$$

Since $\sigma_{11} = 0$,

$$\Delta D_{11} = \frac{-\left(\frac{\nu}{1-2\nu} - \frac{\sigma'_{11}\sigma'_{22}}{\Phi}\right)\Delta D_{22}}{\left(\frac{1-\nu}{1-2\nu} - \frac{\sigma'^2_{11}}{\Phi}\right)}$$

$$\Delta\tau^*_{22} = 2G\left[\left(\frac{\nu}{1-2\nu} - \frac{\sigma'_{11}\sigma'_{22}}{\Phi}\right)\Delta D_{11} + \left(\frac{1-\nu}{1-2\nu} - \frac{\sigma'^2_{22}}{\Phi}\right)\Delta D_{22}\right] \tag{38a}$$

and

$$\Delta\tau^*_{33} = 2G\left[\left(\frac{\nu}{1-2\nu} - \frac{\sigma'_{33}\sigma'_{11}}{\Phi}\right)\Delta D_{11} + \left(\frac{\nu}{1-2\nu} - \frac{\sigma'_{33}\sigma'_{22}}{\Phi}\right)\Delta D_{22}\right] \tag{38b}$$

where the asterisk denotes the Jaumann rate. Then, from eqn (21),

$$\Delta\dot{\sigma}_{22} = \Delta\tau^*_{22} - \sigma_{22}(\Delta D_{11} + \Delta D_{22}) \tag{39a}$$

and

$$\Delta\dot{\sigma}_{33} = \Delta\tau^*_{33} - \sigma_{33}\Delta D_{11}. \tag{39b}$$

At the end of an increment

$$\sigma_{22} \longrightarrow \sigma_{22} + \Delta\dot{\sigma}_{22} \tag{40a}$$

$$\sigma_{33} \longrightarrow \sigma_{33} + \Delta\sigma_{33} \tag{40b}$$

$$L_2 \longrightarrow L_2 + \Delta U_2 \tag{40c}$$

$$L_1 \longrightarrow L_1(1 + \Delta D_{11}). \tag{40d}$$

The instantaneous stiffness matrix is readily computed since the fundamental solution is known from the above algorithm.

A nontrivial solution to the matrix equation (36) exists when the determinant of $[A]$ vanishes. A simple way to determine if this has occurred for a particular guess of U_c, is to perform a Cholesky decomposition of the matrix. Following Needleman[10], a procedure was developed for the program whereby $[A]$ was factored as

$$[A(U_c)] = [L][L]^T \tag{41}$$

where $[L]$ is a lower triangular matrix and $[L]^T$ its transpose. Now the determinant of the stiffness assembly matrix, $|A|$, is given by

$$|A(U_c)| = |L|^2 \tag{42}$$

and since $|L|$ is the product of its diagonal entries, $|A|$ vanishes when one of these diagonal entries is zero. A Newton–Raphson type iteration was employed that determined the smallest value of end displacement, based on successive guesses, for which a diagonal entry of $[L]$, say L_{ii}, vanished. By deleting the ith equation and arbitrarily setting the nodal displacement increment Δu_i^E to unity, the bifurcation mode was calculated.

7. RESULTS AND DISCUSSIONS

As stated previously, the current bifurcation analysis applies to the plane strain deformation of a tension specimen under a uniform displacement and having shear-free ends. The deformation was finite, compressible and elastic–plastic in nature. It was assumed that the material followed a power law strain hardering formula:

$$\epsilon = \frac{\sigma}{E} \qquad \text{for} \quad \sigma < \sigma_y \tag{43a}$$

and

$$\epsilon = \epsilon_y \left(\frac{\sigma}{\sigma_y}\right)^n \quad \text{for} \quad \sigma > \sigma_y \tag{43b}$$

where ϵ_y, σ_y are the yield strain and stress respectively and n is the strain hardening parameter. The stress–strain curves for this study are shown in Fig. 2.

A series of tests was performed with different specimen slenderness ratios corresponding to $L_2^0/L_1^0 = 2, 3$ and 4. A post-bifurcation study was done for the case $L_2^0/L_1^0 = 3, n = 8$. The deformational behavior associated with the rigid grip boundary conditions was also examined with this latter set of parameters.

Analytical results[11, 12] for incompressible elastic–plastic behavior indicate that a diffuse symmetric eigenmode for plane strain bifurcation in the tension test can have the form

$$v_1^E(x_1, x_2) = -Af(x_1)\cos\left(\frac{2\pi x_2}{L_2}\right) \tag{44a}$$

$$v_2^E(x_1, x_2) = B\frac{df(x_1)}{dx}\sin\left(\frac{2\pi x_2}{L_2}\right). \tag{44b}$$

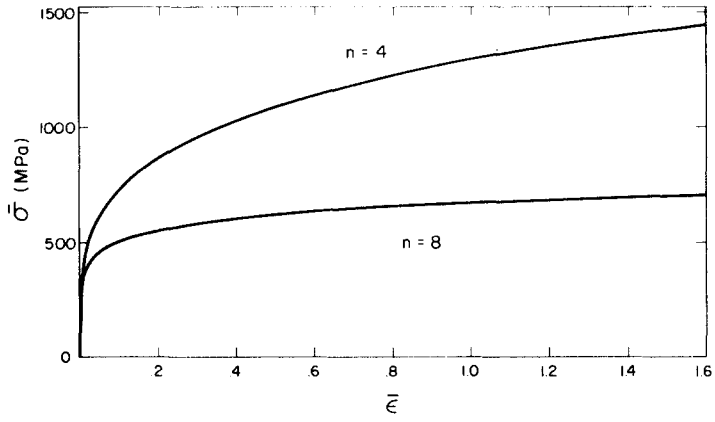

Fig. 2. Idealized material behavior (Ramberg–Osbood formulation, $E = 6.895 \times 10^4$ MPa, $\sigma_y = 344.75$ *MPa*, $\gamma = 1/3$).

When suitably normalized this implies that

$$v_1^E(L_1/x_2) = -\cos\left(\frac{2\pi x_2}{L_2}\right). \tag{44c}$$

For all bifurcation results presented here, the eigenmodes were calculated, and cosine profiles were obtained. Further, it was found in general that the computed eigenfields followed the form of (44) with the best fit for $f(x_1)$ having a sine wave form, i.e.

$$f(x_1) = \alpha \sin\left(\frac{2\pi x_1}{L_2}\right) \tag{45}$$

where α is some constant. For example, in the case $L_2^0/L_1^0 = 4$, $n = 8$, the complete eigenmode was found to approximately satisfy the eqns (44) and (45) with $A = B = 1.807$.

The results of the bifurcation study are given in Table 1. It is observed that as the slenderness ratio is increased the bifurcation point approaches the maximum load point. Hence, in the limit of rather long specimens, the conventional criterion for instability appears valid. When stubbier specimens are used it can be expected, under certain boundary conditions, that necking will be delayed. The rate of strain hardening in the material is also of significance in influencing the bifurcation point. For the same initial slenderness ratios, the ratio U_c/U_m was greater for the larger value of n. Therefore, a material that exhibits a lower strain hardening rate might also exhibit a greater relative increase (ϵ_f/ϵ_m) in strain to failure.

The asymptotic bifurcation formula given by Hill and Hutchinson[12] was particularized to the cases treated here. The value of tangent modulus at the maximum load point, ($dE_t/d\sigma_m$),

Table 1. Plane strain bifurcation in tension. Effect of work hardening rate and slenderness ratio

Slenderness Ratio L_2^0/L_1^0	Work Hardening Exponent n	True Strain at Max. Load ϵ_m	True Strain at Bifurcation ϵ_c	Relative Displacement U_c/U_m
2	4	.254	.334	1.37
2	8	.125	.213	1.77
3	4	.254	.288	1.15
3	8	.125	.162	1.31
4	4	.254	.274	1.09
4	8	.125	.146	1.16

was -6.18 for $n = 8$, and -2.61 for $n = 4$. Hence, the formula is now given by

$$\frac{\sigma_c}{\sigma_m} = 1 + 0.0464\, r^2 \qquad [n = 8] \tag{46a}$$

$$\frac{\sigma_c}{\sigma_m} = 1 + 0.0923\, r^2 \qquad [n = 4] \tag{46b}$$

where $r = \pi(L_2/L_1)_c$ in this instance. The actual ratios from the bifurcation study were compared to those computed from the above equations and the results are given in Table 2.

As previously stated, a post-bifurcation study was done for the case $L_2^0/L_1^0 = 3$, $n = 8$. The necking mode was initiated by arbitrarily choosing a small increment in the fundamental solution ($\Delta U/L_2^0 = 0.01\,\epsilon_y$) and fixing the amplitude of the eigenmode, ξ, so that the increase in effective stress at the point of intersection of the x_2 axis and the top of the bar was virtually zero. Thus, in the first displacement increment from the bifurcation point it was found that

$$\Delta u_2 = 10^{-3}\left(0.15\frac{x_2}{L_2} + 0.1291\,\Delta u_2^E\right). \tag{47}$$

The prescribed increment in end displacement was gradually increased following this perturbation ($0.01\,\epsilon_y \leq \Delta U/L_2^0 < 1.0\,\epsilon_y$).

Table 2. Bifurcation stress

L_2^0/L_1^0	n	σ_c/σ_m (computed)	σ_c/σ_m (eqn 46)
2	4	1.070	1.061
2	8	1.068	1.049
3	4	1.032	1.032
3	8	1.032	1.027
4	4	1.019	1.019
4	8	1.019	1.016

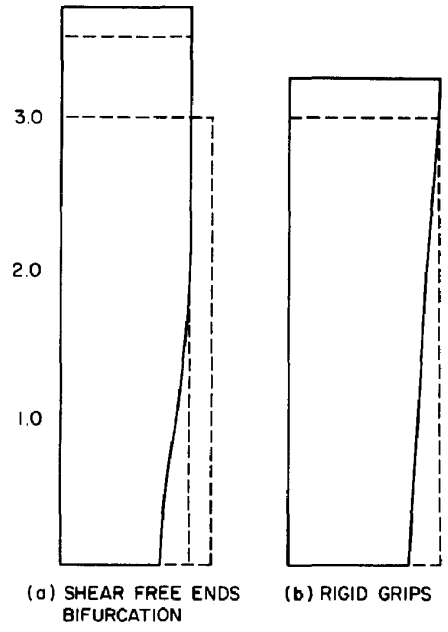

Fig. 3. Shape evolution of rectangular tension specimens—elastic–plastic deformation ($L_2^0/L_1^0 = 3$, $n = 8$).

The shape evolution of the bar from the initial unloaded state is illustrated in Fig. 3(a). With the development of a neck elastic unloading begins in the top of the specimen as shown in Fig. 4(a) and progresses downwards with increased deformation (Fig. 4b). The orientation of the elastic–plastic interface at $U/L_2^0 = 0.24$ is identical to that found by other investigators [19, 25, 26] in their analyses of the large deformation of bars with machined-in necks. A detailed analysis of the stress distribution in the necked region and comparisons to the Bridgman approximation are given in [25, 26]. The greater rate of decrease in the load following bifurcation is illustrated in Fig. 5 where the response is contrasted with that for continued uniform behavior.

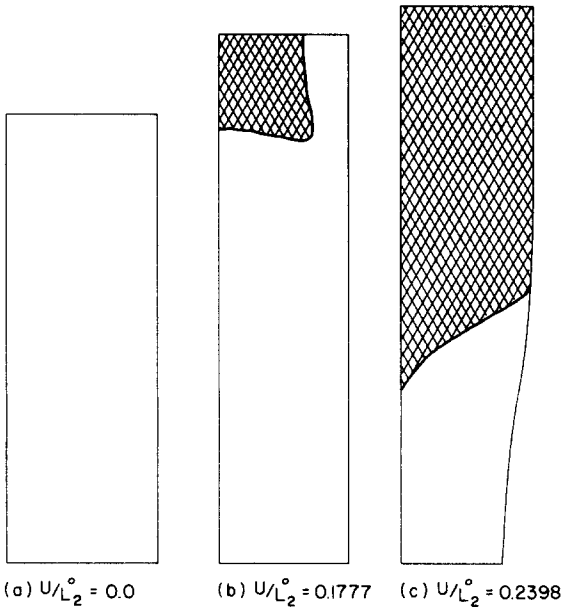

Fig. 4. Post bifurcation development of the elastically unloaded zone in a rectangular tension specimen (shear free ends, $L_2^0/L_1^0 = 3$, $n = 8$).

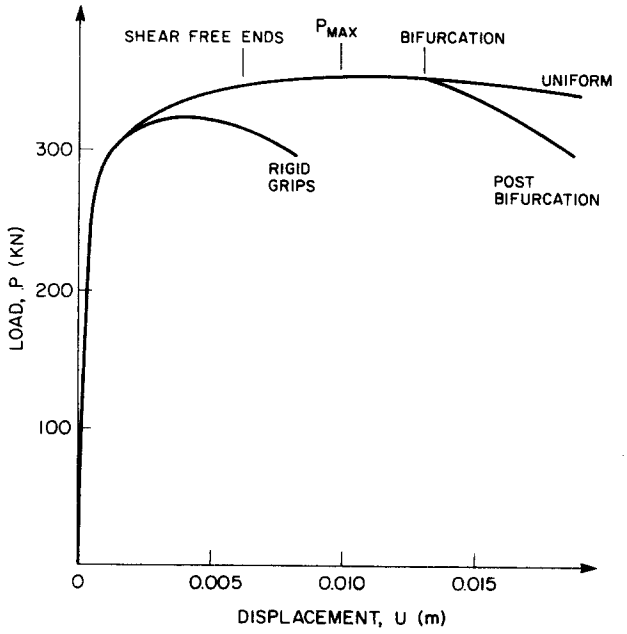

Fig. 5. Load vs displacement of a rectangular tension specimen ($L_2^0 = 0.075$ m, $L_1^0 = 0.025$ m) with (a) shear free ends (uniform and bifurcated solution) and (b) rigid grip conditions.

The study of the deformational behavior of a tension specimen with rigid grip conditions indicated that straining is not uniform even at the outset. The growth of the plastic zone is illustrated in Fig. 6. A plastic zone first develops at the top of the bar as shown in Fig. 6(a). A second zone develops along the longitudinal axis (Fig. 6b) and grows in the manner shown (Fig. 6c, d). Eventually most of the bar deforms plastically with the exception of the region at the top of the bar which never yields (Fig. 6e). With continued extension, the elastically unloaded region extends downwards from this area. As the neck develops and deformation is localized to this region the overall behavior is essentially the same as for the bar with shear-free ends (Fig. 6f). The load-deflection curve for this case is contrasted with that for uniform behavior and with the bifurcation results in Fig. 5. It was noted that the maximum load was approx. 10% less for the rigid grip case and the strain at the point was only 0.432 of the corresponding strain for the shear-free case. The shape evolution is shown in Fig. 3(b) and can be compared with the bifurcated sample. The lateral displacement in the necked region is plotted against extension in Fig 7 and compared with the uniform and bifurcated cases. It is noted that necking develops instantaneously with loading in the rigid grip case. It is expected that a stubbier specimen with these end conditions would have exhibited a certain amount of apparent uniform behavior before necking became observable.

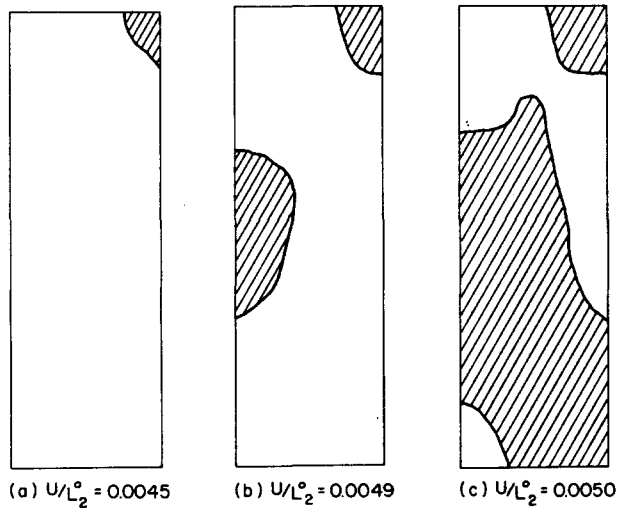

Fig. 6. Development of plastic zones in a rectangular tension specimen with rigid grips ($L_2^0/L_1^0 = 3$, $n = 8$).

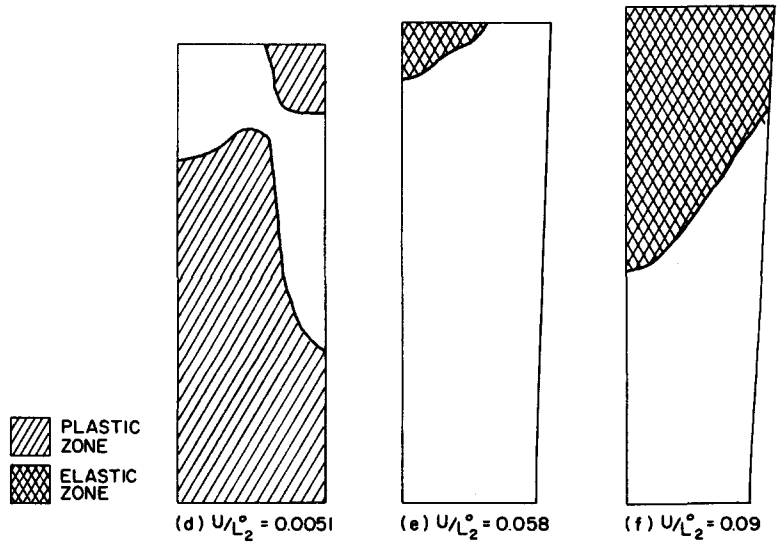

Fig. 6 (*Contd*). Plastically unloaded zones in a rectangular tension specimen with rigid grips.

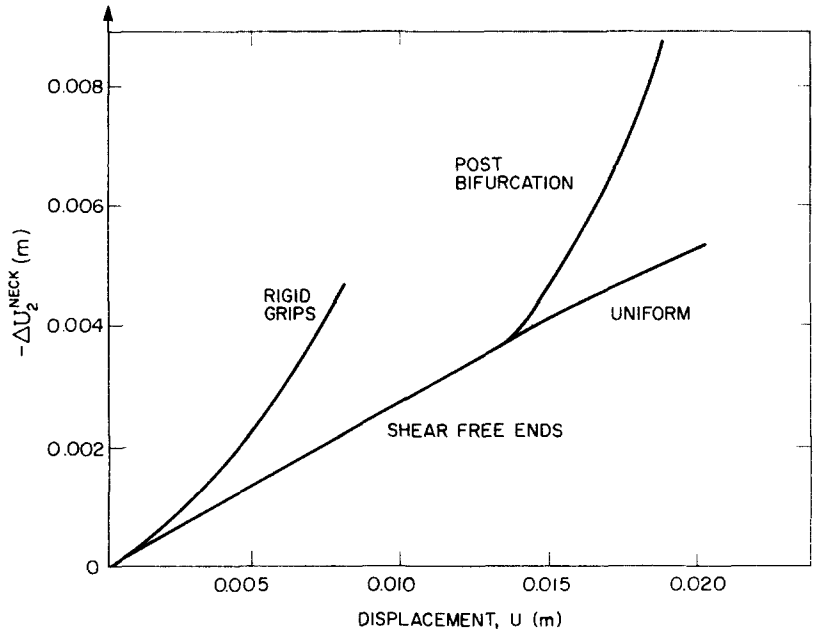

Fig. 7. Displacement in the necked region of a rectangular tension specimen ($L_2^0 = 0.075$ m, $L_1^0 = 0.025$ m) with (a) shear free ends, and (b) rigid grips ($L_2^0/L_1^0 = 3$, $n = 8$).

The simple tension test has been a longstanding means of describing certain parameters associated with the mechanical properties of materials. The study presented here indicates that sometimes results, which are meant to be material constants, can be influenced by various test conditions. Rigid grip conditions produce a nonuniform state of deformation and lead to reduced ductility. On the other hand, if shear-free end conditions can be achieved, specimens with small slenderness ratios could enhance the measured ductility value. The conventional criterion for stability in tension, which was established by Considère[27] in 1885 appears to be a rational one, particularly when inordinately stubby specimens are not used. The condition for necking predicted by this construction is when $d\sigma/d\epsilon = \sigma$ and it appears to provide a lower bound estimate of the point of instability.

Acknowledgements—This work was supported by the National Science Foundation through a Thrust Program on the Application of the Finite Element Method administered by the Center for Materials Research at Stanford. The encouragement and assistance of Prof. E. H. Lee and Dr. R. L. Mallett is gratefully acknowledged.

REFERENCES

1. E. W. Hart, *Acta Met.* **15**, 351–355 (1967).
2. M. A. Burke and W. D. Nix, *Acta Met.* **23**, 793 (1975).
3. R. Hill, *J. Mech. Phys. Solids* **6**, 236–249 (1958).
4. R. Hill, *J. Mech. Phys. Solids* **7**, 209–225 (1959).
5. R. Hill, *J. Mech Phys. Solids* **15**, 371–386 (1967).
6. S. Nemat-Nasser and H. D. Shatoff, *Comput. Structures* **3**, 983–999 (1973).
7. J. W. Hutchinson, *J. Mech. Phys. Solids* **21**, 163–190 (1973).
8. J. P. Miles, *J. Mech. Phys. Solids* **19**, 89–102 (1971).
9. J. W. Hutchinson and J. P. Miles, *J. Mech. Phys. Solids* **22**, 61–71 (1974).
10. A. Needleman, *J. Mech. Phys. Solids* **20**, 111–127 (1972).
11. J. P. Miles, *J. Mech. Phys. Solids* **23**, 197–213 (1975).
12. R. Hill and J. W. Hutchinson, *J. Mech. Phys. Solids* **23**, 239–264 (1975).
13. W. Prager, *Introduction to Mechanics of Continua*, p.155. Dover, New York (1973).
14. Y. C. Fung, *Foundations of Solid Mechanics*, p. 436. Prentice-Hall, Englewood Cliff, New Jersey (1965).
15. R. Hill, *The Mathematical Theory of Plasticity*, p. 15. Oxford University Press (1950).
16. E. H. Lee, R. L. Mallett and W. H. Yang, Stress and Deformation Analysis of the Metal Extrusion Process. Dept. M.E./Div. Appl. Mech. Stanford University Report *SUDAM* No. 76-2 (1976).
17. J. W. Hutchinson, Finite strain analysis of elastic-plastic solids and structures. In *Numerical Solution of Nonlinear Structural Problems* (Edited by R. F. Hartung), AMD, Vol. 6, ASME, New York (1973).
18. E. H. Lee and T. Wierzbicki, *J. Appl. Mech., Trans. ASME* **34**, 931–936 (1967).
19. R. M. McMeeking and J. R. Rice, *Int. J. Solids Structures* **11**, 601–616 (1975).

20. I. Ergatoudis, B. M. Irons and O. C. Zienkiewicz, *Int. J. Solids Structures* **4**, 31–42 (1968).
21. Y. Yamada, N. Yoshimura and T. Sakurai, *Int. J. Mech. Sci.* **10**, 343–354 (1968).
22. R. Hill, *J. Mech. Phys. Solids* **9**, 114–130 (1961).
23. R. Hill, Bifurcation and uniqueness in non-linear mechanics of continua. In *Problems in Continuum Mechanics*, pp. 155–164. SIAM, New York (1961).
24. M. A. Burke, Ph. D. Dissertation, Stanford University (1977).
25. W. H. Chen, *Int. J. Solids Structures* **7**, 685–717 (1972).
26. J. R. Osias, Ph. D. Dissertation, Carnegie-Mellon University (1972).
27. A. Considère, *Ann. Ponts Chaussees*, Ser. 6, **9** p. 574 (1885).